

# Tuning second-order NLO responses through halogen bonding

Elena Cariati,<sup>\*a</sup> Alessandra Forni,<sup>\*b</sup> Serena Biella,<sup>c</sup> Pierangelo Metrangolo,<sup>\*c</sup> Frank Meyer,<sup>c</sup> Giuseppe Resnati,<sup>\*c</sup> Stefania Righetto,<sup>a</sup> Elisa Tordin<sup>a</sup> and Renato Ugo<sup>a</sup>

Receipt/Acceptance Data [DO NOT ALTER/DELETE THIS TEXT]

5 Publication data [DO NOT ALTER/DELETE THIS TEXT]

DOI: 10.1039/b000000x [DO NOT ALTER/DELETE THIS TEXT]

10

## ELECTRONIC SUPPLEMENTARY INFORMATION

---

<sup>a</sup> Dipartimento CIMA and INSTM UdR di Milano and <sup>b</sup>ISTM-CNR, Università di Milano, Via Venezian 21, I-20133 Milano, Italy, Tel: +39 02 5031 4374 (E. C.), 4273 (A. F.); Fax: +39 025031 4405, 4300; E-mail: [elena.cariati@unimi.it](mailto:elena.cariati@unimi.it); [a.forni@istm.cnr.it](mailto:a.forni@istm.cnr.it)

<sup>c</sup> NFM Lab – DCMIC “G. Natta”, Politecnico di Milano, 7, via Mancinelli, I-20131 Milan, Italy, Fax: +39 02 2399 3080; Tel: +39 02 2399 3041 (P. M.), 3032 (G. R.);

E-mail: [pierangelo.metrangolo@polimi.it](mailto:pierangelo.metrangolo@polimi.it); [giuseppe.resnati@polimi.it](mailto:giuseppe.resnati@polimi.it)

† Electronic Supplementary Information (ESI) available: Experimental procedures, characterization, schemes, tables, and details on the theoretical calculations, including a critical discussion of the results, a population analysis of the HOMOs and the LUMOs, and a full description of the simulated spectra; optimized cartesian coordinates of all the examined systems. See <http://dx.doi.org/10.1039/b000000x/>

## Experimental Procedures

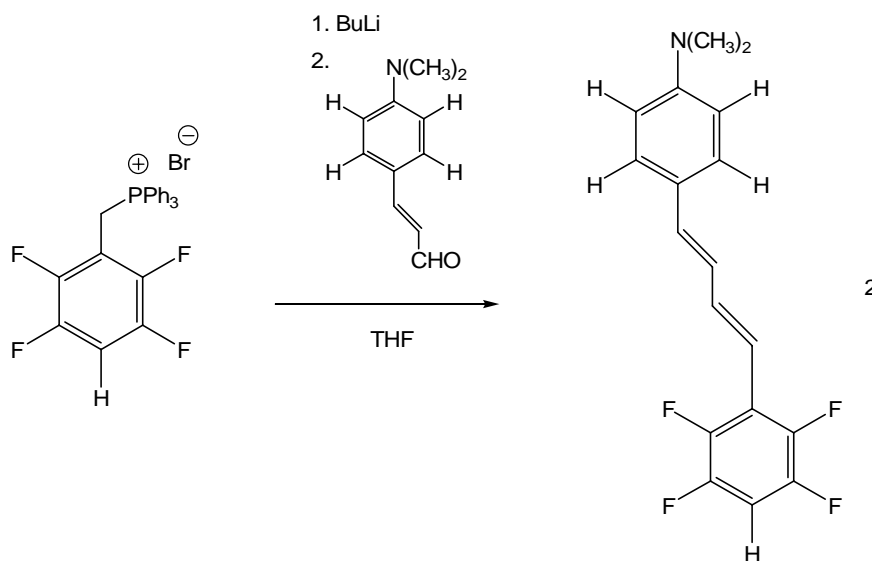
### General

Commercial HPLC-grade solvents were used without further purification. Starting materials were purchased from Sigma–Aldrich, Acros Organics, and Apollo Scientific. Reactions were carried out in oven-dried glassware under a nitrogen atmosphere.  $^1\text{H}$  NMR and  $^{19}\text{F}$  NMR spectra were recorded at ambient temperature with a Bruker AV 500 spectrometer. Unless otherwise stated,  $\text{CDCl}_3$  was used as both solvent and internal standard in  $^1\text{H}$  NMR spectra. For  $^{19}\text{F}$  NMR spectra,  $\text{CDCl}_3$  was used as solvent and  $\text{CFCl}_3$  as internal standard. IR spectra were obtained using a Nicolet Nexus FT-IR spectrometer equipped with UATR unit. UV-vis spectra were recorded on a Jasco V-530 spectrophotometer. Chromatographic separations were performed on silica gel 230-400 mesh. The X-ray crystal structures were determined using a Bruker SMART APEX diffractometer. Melting points were determined with a Reichert instrument by observing the melting and crystallising process through an optical microscope. DSC analyses were carried out with a Linkam DSC600 hot stage (10 °C/min).

### Synthesis of *N,N*-dimethyl-4-[(*E*)-2-(2,3,5,6-tetrafluoro-4-iodophenyl)vinyl]aniline (**1a**).

See ref. 4.

### Synthesis of *N,N*-dimethyl-4-[(1*E*,3*E*)-4-(2,3,5,6-tetrafluorophenyl)buta-1,3-dien-1-yl]aniline (**2**).

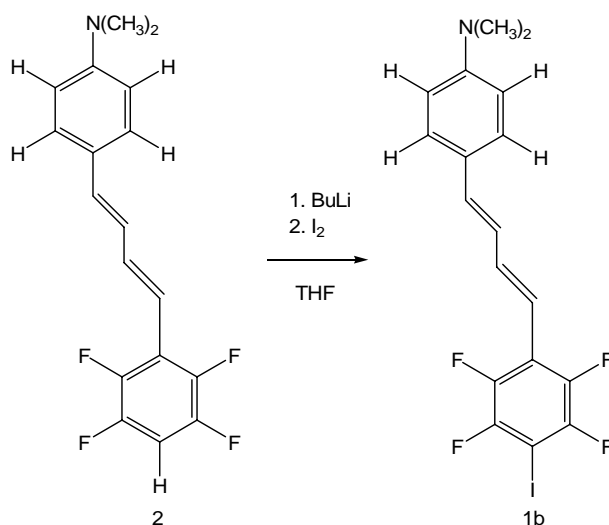


1.40 Mmol of BuLi (1.6 M) are added to a solution of 700 mg (1.17 mmol) of phosphonium bromide in 4 mL of THF at  $-70^\circ\text{C}$ . Then the mixture is warmed up to room temperature, and the solution turns red/black. After 30min, 367 mg (2.10 mmol) of aldehyde are added and the solution is stirred during 24h. Then, the solution is hydrolysed with  $\text{NH}_4\text{Cl}$  and the aqueous phase is extracted 3 times with  $\text{CH}_2\text{Cl}_2$ . The organic layer is dried over  $\text{Na}_2\text{SO}_4$ . The crude material was chromatographed with hexane/ $\text{CH}_2\text{Cl}_2$  1/1 as eluent to give 350 mg of product **2** as a yellow powder (93% yield).

---

M.p. = 140-142°C;  $^1\text{H}$  NMR (500 MHz,  $\text{CDCl}_3$ ) :  $\delta$  7.37 (2H, d,  $J = 8.8$ , H arom.), 7.33 (1H, dd,  $J = 9.5$ ,  $J = 15.9$ , CH), 6.86 (1H, m, H arom.), 6.79 (1H, dd,  $J = 9.5$ ,  $J = 15.5$ , CH), 6.73 (1H, d,  $J = 15.5$ , CH), 6.71 (2H, d,  $J = 8.8$ , H arom.), 6.55 (1H, d,  $J = 15.5$ , CH), 3.02 (6H, s,  $\text{CH}_3$ ) ;  $^{19}\text{F}$  NMR (470 MHz,  $\text{CDCl}_3$ ) :  $\delta$  -144.4 (2F, m), -141.2 (2F, m). GC-MS 321 ( $\text{M}^+$ ).

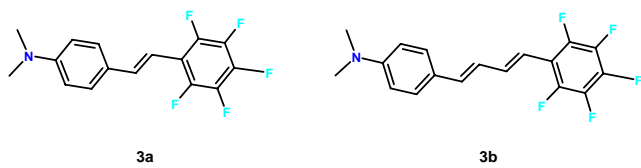
Synthesis of *N,N*-dimethyl-4-[(1*E*,3*E*)-4-(2,3,5,6-tetrafluoro-4-iodophenyl)buta-1,3-dien-1-yl]aniline (**1b**).



365 Mg (1.14 mmol) of compound were stirred in 5 mL of THF at  $-70^{\circ}\text{C}$ . 1.48 mmol of BuLi (1.6 M) are added and the mixture is warmed up to room temperature. After 30min, the reaction is cooled down at  $-70^{\circ}\text{C}$  and a solution of 376 mg (1.48 mmol) of  $\text{I}_2$  in 1mL of THF is added. After 2h, the solution is warmed up and 439 mg of compound **1b** are filtered off as a yellow powder (86% yield).

M.p. =  $228\text{-}234^{\circ}\text{C}$ ;  $^1\text{H}$  NMR (500 MHz,  $\text{CDCl}_3$ ) :  $\delta$  7.36 (2H, d,  $J = 8.7$ , H arom.), 7.32 (1H, m, CH), 6.76 (2H, m, CH), 6.69 (2H, d,  $J = 8.7$ , H arom.), 6.50 (1H, d,  $J = 15.9$ , CH), 3.00 (6H, s,  $\text{CH}_3$ ) ;  $^{19}\text{F}$  NMR (470 MHz,  $\text{CDCl}_3$ ) :  $\delta$  -142.1 (2F, m), -123.1 (2F, m). MS (ESI)  $m/z$  447.8 ( $\text{M}+\text{H}$ ) $^+$ .

*Scheme 2.*



<sup>19</sup>F NMR Experiments.

The samples were prepared by addition of 100 eq. of XB-acceptor solvents to 0.5 mL of a solution 5x10<sup>-3</sup> M of **1b** in CDCl<sub>3</sub>. Chemical shifts were recorded by using CFC<sub>3</sub> as external reference.

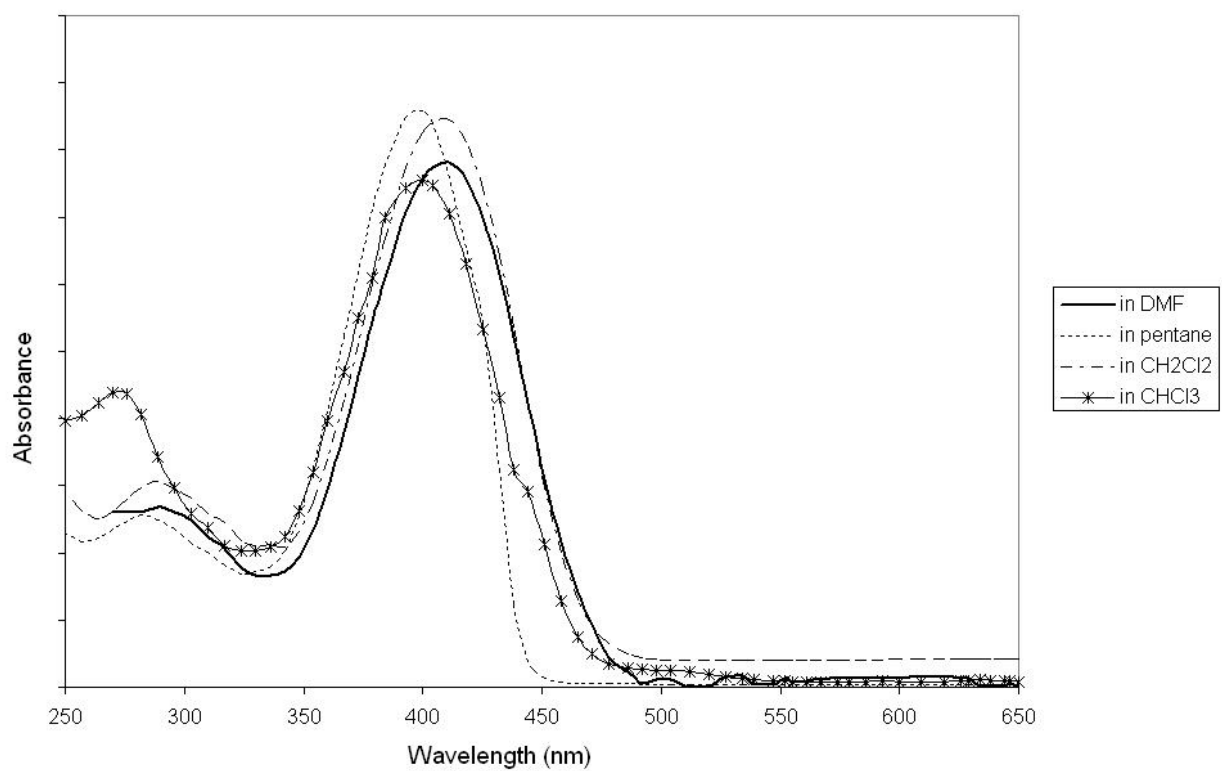
**Table 3.**

XB-acceptor solvent	$\Delta\delta^a = \delta_{\mathbf{1b}} \text{ in CHCl}_3 - \delta_{\text{used solvent}}$	$\Delta\delta^b = \delta_{\mathbf{1b}} \text{ in CHCl}_3 - \delta_{\text{used solvent}}$
-	-	-
QUI	0.65	0.54
PIP	0.28	0.20
DMF	0.08	0.09
Dioxane	0.04	0.04
2,2',5,5'-tetramethyl-PIP	0.03	0.07

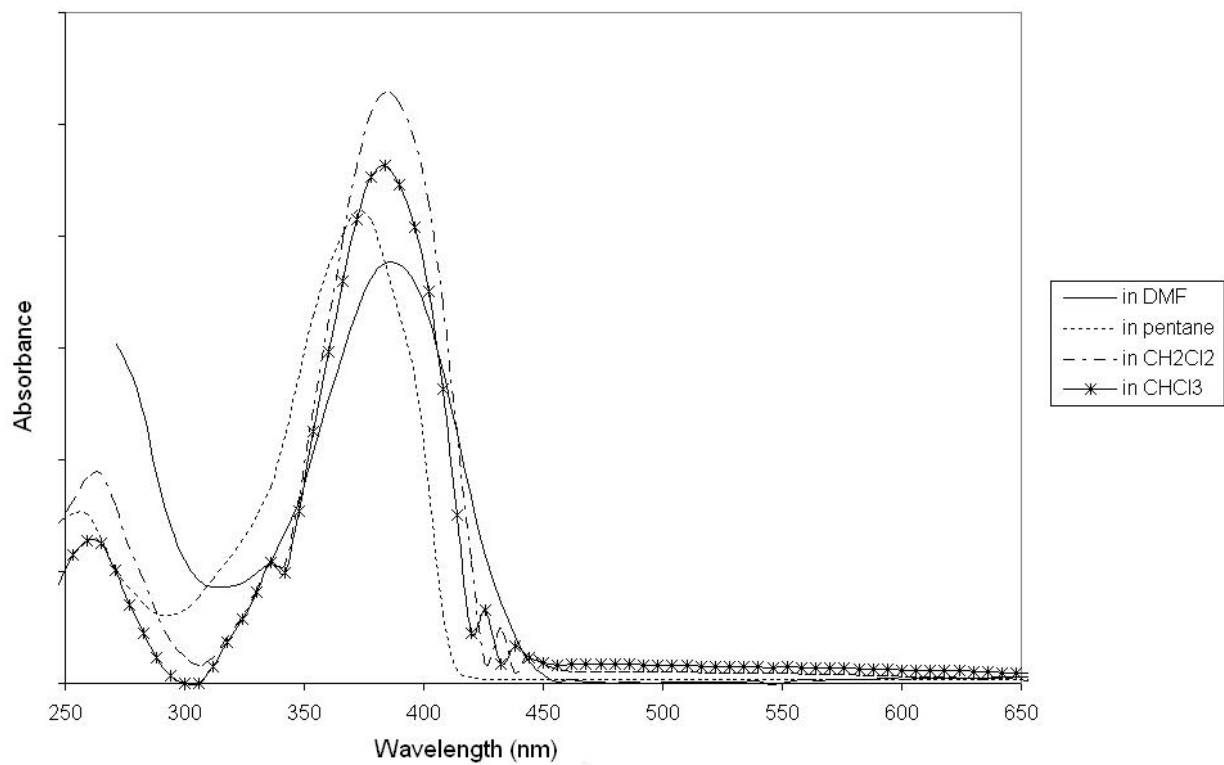
<sup>a</sup>: variation calculated on the peak at -123.1 ppm (see above);

<sup>b</sup>: variation calculated on the peak at -142.1 ppm (see above).

*UV-vis absorption spectra*



UV-vis absorption spectra of compound **1b** in different solvents



UV-vis absorption spectra of compound **2** in different solvents



## Details on DFT and TDDFT calculations

Geometry optimisations<sup>8</sup> of compounds **1a**, **1b**, **2** and of dimers of **1a** with DMF (**1a**·DMF), piperidine (**1a**·PIP) and quinuclidine (**1a**·QUI) were performed within the DFT approach, using the B3LYP functional and the 3-21G\*\* basis set. The good agreement between computed and experimental, when available, bond lengths (see Table 4 and Figure S1 for atom numbering) indicates the suitability of the chosen approach, in spite of the relatively small basis set (due to unavailability of larger basis set for iodine). Moreover, in the case of compound **2**, lacking of iodine, we performed another geometry optimisation with the 6-31G\*\* basis set, obtaining a dipole moment, 5.89 D, very similar to the one determined with the 3-21G\*\* basis set (6.10 D). In Tables 10-15 the optimised B3LYP/3-21G\*\* Cartesian coordinates of all investigated systems are reported.

The optimised geometries of **1a**, **1a**·DMF, **1a**·PIP and **1a**·QUI were then used for TDDFT calculations<sup>7</sup> of electronic spectra and hyperpolarizability tensors,  $\beta$ . These calculations were performed with the ADF triple-zeta polarized Slater-type orbital basis set ‘TZP’ for all atoms, using the Van Leeuwen–Baerends (LB94) exchange-correlation potential. The quantity  $\beta_\lambda$  was derived from the  $\beta_{ijk}$  elements according to  $\beta_\lambda = (\mu_x\beta_x + \mu_y\beta_y + \mu_z\beta_z)/\mu$ , where  $\beta_i = \beta_{iii} + (1/3)\sum_{j\neq i}(\beta_{ijj} + \beta_{jji} + \beta_{jji})$  are the components of vector  $\beta_{tot}$ . The ADF  $\beta_{ijk}$  components already converted to be compared with the experimental values have been used.<sup>S1</sup>

The properties of the more significant transitions (i.e. with  $f > 0.05$ ,  $f$  being the oscillator strength) for **1a**, **1a**·DMF, **1a**·PIP and **1a**·QUI are reported in Table 5. In all cases, the HOMO→LUMO appears as the most significant transition at  $\lambda=445$ , 454, 448 and 447 nm for **1a**, **1a**·DMF, **1a**·PIP and **1a**·QUI, respectively (see Tables 6-9 for a population analysis of the HOMO and the LUMO of each optimised structure). The observed difference between the calculated and the experimental transition energies, amounting to 0.46 eV for **1a**, is in the range of the errors normally found when computing electronic spectra of relatively large systems.<sup>S2</sup> Besides the HOMO→LUMO transition, the computed spectra show essentially other two minor transitions at higher energies. The former one (at  $\lambda=357$ , 383, 376 and 374 nm for **1a**, **1a**·DMF, **1a**·PIP and **1a**·QUI, respectively) is principally a HOMO-1→LUMO transition, where the HOMO-1 is a  $\pi$  orbital essentially localized on the iodine atom. The latter one (at  $\lambda=301$ -302 nm for all systems) is a transition from a  $\pi$  orbital localized on I, N and the ethylenic bond towards the LUMO. The experimental spectrum of **1a** in chloroform showed only the former of these minor transitions, due to the solvent cut off, as a very weak band at 288 nm.

For each of the dimers **1a**·DMF and **1a**·PIP, another transition was obtained, which is very close to, and partially mixed with the HOMO→LUMO transition for **1a**·DMF ( $\lambda=442$  nm) and the HOMO-1→LUMO transition for **1a**·PIP ( $\lambda=367$  nm). Clearly, in both cases the two transitions are too close to be resolved in the experimental spectra. In the case of **1a**·DMF, this further transition is a HOMO→LUMO+1, where the LUMO+1 describes the  $\pi^*$  system of DMF. For the dimer **1a**·PIP, it is a transition from a  $\sigma$  orbital localized on the nitrogen atom of piperidine towards the LUMO.

Finally, it is to be noted that, from calculations, the only electronic transition showing a significant change due to XB formation is the intermediate one, which shifts in all cases towards lower energies, still maintaining its HOMO-1→LUMO character. Experimentally this weak band cannot be seen other than in chloroform. The computed red-shift is slightly more pronounced for DMF ( $\Delta\lambda=26$ nm) with respect to piperidine and quinuclidine ( $\Delta\lambda=19$  and 17nm, respectively), in

apparent contrast with the computed trend of the XB interaction strength, indicating that no simple relation does exist between the two quantities.

## References

(8) (full reference) Frisch, M. J.; Trucks, G. W.; Schlegel, H. B.; Scuseria, G. E.; Robb, M. A.; Cheeseman, J. R.; Zakrzewski, V. G.; Montgomery Jr., J. A.; Stratmann, R. E.; Burant, J. C.; Dapprich, S.; Millam, J. M.; Daniels, A. D.; Kudin, K. N.; Strain, M. C.; Farkas, O.; Tomasi, J.; Barone, V.; Cossi, M.; Cammi, R.; Mennucci, B.; Pomelli, C.; Adamo, C.; Clifford, S.; Ochterski, J.; Petersson, G. A.; Ayala, P. Y.; Cui, Q.; Morokuma, K.; Malick, D. K.; Rabuck, A. D.; Raghavachari, K.; Foresman, J. B.; Cioslowski, J.; Ortiz, J. V.; Baboul, A. G.; Stefanov, B. B.; Liu, G.; Liashenko, A.; Piskorz, P.; Komaromi, I.; Gomperts, R.; Martin, R. L.; Fox, D. J.; Keith, T.; Al-Laham, M. A.; Peng, C. Y.; Nanayakkara, A.; Challacombe, M.; Gill, P. M. W.; Johnson, B.; Chen, W.; Wong, M. W.; Andres, J. L.; Gonzalez, C.; Head-Gordon, M.; Replogle, E. S.; Pople, J. A. *Gaussian 98*, Revision A.11.3; Gaussian, Inc.: Pittsburgh, PA, **2002**.

(S1) Willets, A.; Rice, J. E.; Burland, D. M.; Shelton, D. P. *J. Chem. Phys.*, **1992**, *97*, 7590-7599).

(S2) Grimme S. *Calculation of the Electronic Spectra of Large Molecules*. In *Reviews in Computational Chemistry, Vol. 20*; Lipkowitz, K. B., Larter, R., Cundari, T. R., Eds.; Wiley-VCH: New York, **2004**.

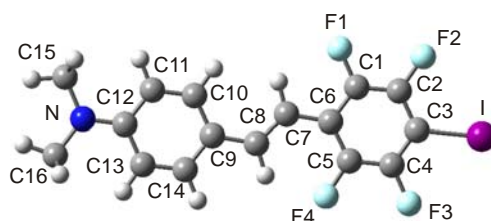


**Figure S1.** B3LYP/3-21G\*\* optimized geometry of compound **1a** with atom numbering.

**Table 4.**

Selected geometrical parameters in optimised B3LYP/3-21G\*\* structures of **1a**, **1b**, **2** and dimers **1a**·DMF, **1a**·PIP, **1a**·QUI, compared with experimental data<sup>4</sup> (in parentheses) if available. Bond lengths in Ångström.

	<b>1a</b>	<b>1b</b>	<b>2</b>	<b>1a</b> ·DMF	<b>1a</b> ·PIP	<b>1a</b> ·QUI
I–C3	2.110 (2.087) <sup>a</sup>	2.110 (2.080) <sup>b</sup>		2.129	2.152	2.154
C1–F1	1.371 (1.347)	1.370 (1.350)	1.370	1.373	1.373	1.373
C2–F2	1.363 (1.340)	1.363 (1.346)	1.365	1.367	1.368	1.368
C4–F3	1.364 (1.352)	1.364 (1.341)	1.366	1.367	1.368	1.368
C5–F4	1.373 (1.344)	1.373 (1.342)	1.373	1.375	1.376	1.376
C7–C8	1.354 (1.331)	1.358 (1.338)	1.357	1.352	1.352	1.352
N–C <sub>ar</sub>	1.378 (1.389)	1.379 (1.387)	1.379	1.381	1.381	1.381
I...O(N)				2.668	2.688	2.678

<sup>a</sup> Experimental data from ref. 4; <sup>b</sup> experimental data to be published.

**Table 5.**

Computed TDDFT spectra of **1a** and its dimers with DMF, piperidine and quinuclidine: wavelengths ( $\lambda$ , nm), oscillator strengths (f) and transition dipole moments ( $\mu_{eg}$ , D).

<b>1a</b>			<b>1a</b> · DMF			<b>1a</b> · PIP			<b>1a</b> · QUI		
$\lambda$	f	$\mu_{eg}$	$\lambda$	f	$\mu_{eg}$	$\lambda$	f	$\mu_{eg}$	$\lambda$	f	$\mu_{eg}$
445	0.97	9.59	454	0.76	8.54	448	1.11	10.30	447	1.14	10.39
			442	0.34	5.66						
357	0.25	4.39	383	0.08	2.48	376	0.06	2.12	374	0.12	3.06
						367	0.06	2.25			
301	0.37	4.87	302	0.39	4.99	301	0.47	5.48	302	0.61	6.26

**Table 6.**

Populations (%) of the Molecular Orbitals (MO) principally involved (weight=0.91) in the strongest TDDFT transition of compound **1a** ( $\lambda=445$  nm,  $f=0.97$ , see Table 5). Atom numbering (in parentheses) as in Figure S1.

E(eV)	Occupation	MO	%	Atomic Orbital	Atom			
-10.045	2.00(HOMO)	63 A	25.01%	1 P:z	34 N(N)			
			13.72%	1 P:z	10 C(C9)			
			12.90%	1 P:z	2 C(C7)			
			8.60%	1 P:z	12 C(C13)			
			7.19%	1 P:z	14 C(C11)			
			6.00%	1 P:z	13 C(C12)			
			3.62%	1 P:z	7 C(C3)			
			3.18%	1 P:z	1 I(I)			
			2.72%	1 P:z	9 C(C1)			
			2.72%	1 P:z	5 C(C5)			
			1.77%	1 P:z	15 C(C10)			
			-7.988	0.00(LUMO)	64 A	20.75%	1 P:z	3 C(C8)
						15.90%	1 P:z	7 C(C3)
						12.22%	1 P:z	4 C(C6)
8.28%	1 P:z	5 C(C5)						
7.53%	1 P:z	2 C(C7)						
6.67%	1 P:z	13 C(C12)						
6.63%	1 P:z	15 C(C10)						
4.72%	1 P:z	9 C(C1)						
4.67%	1 P:z	11 C(C14)						
3.77%	1 P:z	8 C(C2)						
3.51%	1 P:z	34 N(N)						
2.60%	1 P:z	1 I(I)						

**Table 7.**

Populations (%) of the Molecular Orbitals (MO) principally involved (weight=0.64) in the strongest TDDFT transition of dimer **1a** -DMF ( $\lambda=454$  nm,  $f=0.76$ , see Table 5). Atom numbering (in parentheses) as in Figure S1.

E(eV)	Occupation	MO	%	Atomic Orbital	Atom			
-9.732	2.00(HOMO)	78 A	22.61%	1 P:z	44 N(N)			
			12.73%	1 P:z	2 C(C7)			
			12.53%	1 P:z	10 C(C9)			
			7.64%	1 P:z	12 C(C13)			
			6.43%	1 P:z	14 C(C11)			
			6.18%	1 P:z	1 I(I)			
			6.15%	1 P:z	13 C(C12)			
			3.75%	1 P:z	7 C(C3)			
			2.78%	1 P:z	9 C(C1)			
			-7.571	0.00(LUMO)	79 A	20.63%	1 P:z	3 C(C8)
						14.45%	1 P:z	7 C(C3)
10.25%	1 P:z	4 C(C6)						
9.75%	1 P:z	2 C(C7)						
8.34%	1 P:z	5 C(C5)						
7.39%	1 P:z	15 C(C10)						
7.35%	1 P:z	13 C(C12)						
4.98%	1 P:z	9 C(C1)						
4.70%	1 P:z	11 C(C14)						
3.45%	1 P:z	44 N(N)						
2.71%	1 P:z	8 C(C2)						
2.59%	1 P:z	1 I(I)						

**Table 8.**

Populations (%) of the Molecular Orbitals (MO) principally involved (weight=0.93) in the strongest TDDFT transition of dimer **1a** ·PIP ( $\lambda=448$  nm,  $f=1.11$ , see Table 5). Atom numbering (in parentheses) as in Figure S1.

E(eV)	Occupation	MO	%	Atomic Orbital	Atom			
-9.746	2.00 (HOMO)	81 A	23.21%	1 P:z	50 N(N)			
			12.95%	1 P:z	2 C(C7)			
			12.84%	1 P:z	10 C(C9)			
			7.87%	1 P:z	12 C(C13)			
			6.60%	1 P:z	14 C(C11)			
			6.22%	1 P:z	13 C(C12)			
			4.31%	1 P:z	1 I(I)			
			3.89%	1 P:z	7 C(C3)			
			2.81%	1 P:z	9 C(C1)			
			2.76%	1 P:z	5 C(C5)			
			2.49%	1 P:z	3 C(C8)			
			2.11%	1 P:z	15 C(C10)			
			2.00%	1 P:z	11 C(C14)			
			-7.568	0.00 (LUMO)	82 A	20.67%	1 P:z	3 C(C8)
						14.46%	1 P:z	7 C(C3)
						10.16%	1 P:z	4 C(C6)
9.95%	1 P:z	2 C(C7)						
8.38%	1 P:z	5 C(C5)						
7.44%	1 P:z	15 C(C10)						
7.40%	1 P:z	13 C(C12)						
5.02%	1 P:z	9 C(C1)						
4.72%	1 P:z	11 C(C14)						
3.45%	1 P:z	50 N(N)						
2.67%	1 P:z	8 C(C2)						
2.12%	1 P:z	1 I(I)						

**Table 9.**

Populations (%) of the Molecular Orbitals (MO) principally involved (weight=0.93) in the strongest TDDFT transition of dimer **1a** ·QUI ( $\lambda=447$  nm,  $f=1.14$ , see Table 5). Atom numbering (in parentheses) as in Figure S1.

E(eV)	Occupation	MO	%	Atomic Orbital	Atom			
-9.730	2.00 (HOMO)	86 A	23.12%	1 P:z	54 N(N)			
			12.98%	1 P:z	2 C(C7)			
			12.81%	1 P:z	10 C(C9)			
			7.83%	1 P:z	12 C(C13)			
			6.57%	1 P:z	14 C(C11)			
			6.25%	1 P:z	13 C(C12)			
			4.48%	1 P:z	1 I(I)			
			3.91%	1 P:z	7 C(C3)			
			2.83%	1 P:z	9 C(C1)			
			2.77%	1 P:z	5 C(C5)			
			2.58%	1 P:z	3 C(C8)			
			2.14%	1 P:z	15 C(C10)			
			2.03%	1 P:z	11 C(C14)			
			-7.546	0.00 (LUMO)	87 A	20.70%	1 P:z	3 C(C8)
						14.38%	1 P:z	7 C(C3)
						10.12%	1 P:z	2 C(C7)
10.07%	1 P:z	4 C(C6)						
8.38%	1 P:z	5 C(C5)						
7.51%	1 P:z	15 C(C10)						

7.47%	1 P:z	13 C(C12)
5.05%	1 P:z	9 C(C1)
4.73%	1 P:z	11 C(C14)
3.47%	1 P:z	54 N(N)
2.62%	1 P:z	8 C(C2)
2.10%	1 P:z	1 I(I)

**Table 10.**

Optimized B3LYP/3-21G\*\* coordinates for compound **1a**

Standard orientation:

Center Number	Atomic Number	Atomic Type	Coordinates (Angstroms)		
			X	Y	Z
1	53	0	5.356173	-0.118003	0.000034
2	6	0	-1.000504	0.439274	-0.000026
3	1	0	-1.281931	1.482583	0.000029
4	6	0	-1.950566	-0.525090	-0.000087
5	1	0	-1.631505	-1.556496	-0.000137
6	6	0	0.438714	0.232649	-0.000035
7	6	0	1.083963	-1.010633	0.000036
8	6	0	2.468253	-1.110559	0.000050
9	6	0	3.251836	0.035458	-0.000005
10	6	0	2.641397	1.282858	-0.000081
11	6	0	1.259479	1.371143	-0.000096
12	9	0	0.353657	-2.173762	0.000115
13	9	0	3.051442	-2.343541	0.000148
14	9	0	3.394021	2.419240	-0.000151
15	9	0	0.668042	2.607537	-0.000171
16	6	0	-3.391131	-0.312909	-0.000078
17	6	0	-4.245652	-1.433702	-0.000071
18	1	0	-3.810457	-2.424522	-0.000080
19	6	0	-5.626443	-1.306224	-0.000027
20	1	0	-6.232063	-2.198195	0.000025
21	6	0	-6.240327	-0.028846	0.000020
22	6	0	-5.380397	1.101651	-0.000026
23	1	0	-5.798015	2.095742	-0.000096
24	6	0	-4.003202	0.957732	-0.000068
25	1	0	-3.391891	1.849211	-0.000124
26	7	0	-7.611544	0.112059	0.000087
27	6	0	-8.476289	-1.078860	-0.000466
28	1	0	-8.308123	-1.697722	-0.887318
29	1	0	-9.515898	-0.758641	-0.001005
30	1	0	-8.309075	-1.697950	0.886416
31	6	0	-8.220801	1.451788	0.000627
32	1	0	-7.933565	2.025393	0.887377
33	1	0	-9.303426	1.345027	0.001405
34	1	0	-7.934831	2.025676	-0.886368

**Table 11.**

Optimized B3LYP/3-21G\*\* coordinates for compound **1b**

Standard orientation:

Center Number	Atomic Number	Atomic Type	Coordinates (Angstroms)		
			X	Y	Z
1	53	0	-6.305466	-0.264895	0.000070
2	9	0	-1.169422	-1.958964	-0.000053
3	9	0	-3.848137	-2.321278	0.000038
4	9	0	-4.528689	2.405272	-0.000014
5	9	0	-1.823805	2.787020	-0.000131
6	6	0	-1.981094	-0.851938	-0.000048
7	6	0	-3.354446	-1.050084	0.000002
8	6	0	-4.217502	0.037449	0.000012
9	6	0	-3.697014	1.325202	-0.000028
10	6	0	-2.324948	1.512347	-0.000084
11	6	0	-1.425768	0.434327	-0.000097

12	6	0	-0.006089	0.735877	-0.000167
13	1	0	0.219542	1.793658	-0.000286
14	6	0	1.014640	-0.159645	-0.000092
15	1	0	0.790092	-1.215907	0.000037
16	6	0	2.402317	0.224377	-0.000165
17	1	0	2.620544	1.286373	-0.000374
18	6	0	3.409326	-0.686638	-0.000011
19	1	0	3.133235	-1.737188	0.000104
20	6	0	4.840441	-0.428335	-0.000001
21	6	0	5.405666	0.864814	0.000488
22	1	0	4.761624	1.732929	0.001029
23	6	0	6.776792	1.059968	0.000452
24	1	0	7.157122	2.068943	0.001013
25	6	0	7.678634	-0.037042	-0.000102
26	6	0	7.112660	-1.336443	-0.000501
27	1	0	7.751222	-2.205107	-0.000940
28	6	0	5.737942	-1.516180	-0.000453
29	1	0	5.341534	-2.523270	-0.000818
30	7	0	9.043976	0.154566	-0.000189
31	6	0	9.952307	-1.003391	0.000784
32	1	0	9.806912	-1.628192	0.887552
33	1	0	10.979309	-0.644690	0.001779
34	1	0	9.808680	-1.628433	-0.886122
35	6	0	9.603203	1.515910	-0.000383
36	1	0	10.689042	1.449240	-0.002172
37	1	0	9.296915	2.078345	0.887182
38	1	0	9.294145	2.078898	-0.886599

**Table 12.**

Optimized B3LYP/3-21G\*\* coordinates for compound **2**

Standard orientation:

Center Number	Atomic Number	Atomic Type	Coordinates (Angstroms)		
			X	Y	Z
1	1	0	-7.258694	-0.408127	0.000137
2	9	0	-3.093916	-2.142585	-0.000270
3	9	0	-5.768931	-2.570651	-0.000152
4	9	0	-6.570221	2.129857	0.000330
5	9	0	-3.870533	2.586192	0.000203
6	6	0	-3.936079	-1.057661	-0.000122
7	6	0	-5.305080	-1.286035	-0.000062
8	6	0	-6.197080	-0.225642	0.000090
9	6	0	-5.707662	1.071334	0.000178
10	6	0	-4.341182	1.299127	0.000115
11	6	0	-3.416906	0.243042	-0.000035
12	6	0	-2.003796	0.581276	-0.000086
13	1	0	-1.806155	1.644732	-0.000047
14	6	0	-0.959818	-0.285890	-0.000155
15	1	0	-1.154532	-1.348067	-0.000180
16	6	0	0.417112	0.138474	-0.000180
17	1	0	0.602606	1.206714	-0.000201
18	6	0	1.451855	-0.739995	-0.000169
19	1	0	1.210321	-1.798982	-0.000177
20	6	0	2.874500	-0.434077	-0.000138
21	6	0	3.395184	0.877361	0.000132
22	1	0	2.721949	1.723077	0.000386
23	6	0	4.759036	1.119412	0.000174
24	1	0	5.104684	2.140805	0.000506
25	6	0	5.697751	0.054153	-0.000072
26	6	0	5.176746	-1.263490	-0.000305
27	1	0	5.844772	-2.109697	-0.000522
28	6	0	3.808603	-1.490348	-0.000340
29	1	0	3.446811	-2.510431	-0.000546
30	7	0	7.056252	0.293010	-0.000050
31	6	0	8.004477	-0.832137	0.000852
32	1	0	7.881699	-1.461936	0.887639
33	1	0	9.018300	-0.437426	0.001600
34	1	0	7.883121	-1.462274	-0.885900
35	6	0	7.567198	1.672961	-0.000250
36	1	0	8.654745	1.644497	-0.001453
37	1	0	7.240863	2.224676	0.886973
38	1	0	7.238999	2.224859	-0.886640

**Table 13.**

Optimized B3LYP/3-21G\*\* coordinates for dimer **1a**-DMF

Standard orientation:

Center Number	Atomic Number	Atomic Type	Coordinates (Angstroms)		
			X	Y	Z
1	53	0	3.758397	-0.272694	-0.006939
2	6	0	-2.612902	0.433096	-0.001835
3	1	0	-2.873300	1.482147	-0.002108
4	6	0	-3.580450	-0.511818	-0.000255
5	1	0	-3.280356	-1.548774	-0.000047
6	6	0	-1.175979	0.198132	-0.003299
7	6	0	-0.556734	-1.057543	-0.003349
8	6	0	0.825303	-1.182792	-0.004748
9	6	0	1.640509	-0.059215	-0.006103
10	6	0	1.048529	1.196489	-0.006166
11	6	0	-0.331387	1.318012	-0.004758
12	9	0	-1.313149	-2.205989	-0.002077
13	9	0	1.377430	-2.432871	-0.004750
14	9	0	1.820879	2.323895	-0.007593
15	9	0	-0.898698	2.568036	-0.004833
16	6	0	-5.019338	-0.273937	0.001276
17	6	0	-5.892071	-1.379814	0.002843
18	1	0	-5.472976	-2.377572	0.002835
19	6	0	-7.271347	-1.229831	0.004415
20	1	0	-7.891030	-2.112193	0.005505
21	6	0	-7.864175	0.056488	0.004496
22	6	0	-6.986479	1.172111	0.002930
23	1	0	-7.387826	2.173003	0.003009
24	6	0	-5.610738	1.005700	0.001362
25	1	0	-4.984429	1.886802	0.000231
26	7	0	-9.235201	0.219139	0.006060
27	6	0	-10.117052	-0.957965	0.007983
28	1	0	-9.960453	-1.580772	-0.878521
29	1	0	-11.152003	-0.622479	0.009413
30	1	0	-9.957730	-1.579844	0.894644
31	6	0	-9.822421	1.567572	0.005722
32	1	0	-9.526342	2.138077	0.891840
33	1	0	-10.906803	1.478430	0.006436
34	1	0	-9.527469	2.137043	-0.881428
35	8	0	6.414776	-0.521887	0.001498
36	6	0	7.192592	0.459139	0.004289
37	1	0	6.843421	1.495418	0.000333
38	7	0	8.543629	0.352367	0.012417
39	6	0	9.417375	1.533531	0.015598
40	1	0	8.805862	2.436238	0.010179
41	1	0	10.049167	1.542266	0.907081
42	1	0	10.060049	1.538892	-0.868078
43	6	0	9.165361	-0.986330	0.019037
44	1	0	9.789892	-1.119004	-0.866932
45	1	0	9.778780	-1.115316	0.913272
46	1	0	8.351588	-1.708771	0.015431

**Table 14.**

Optimized B3LYP/3-21G\*\* coordinates for dimer **1a**-PIP

Standard orientation:

Center Number	Atomic Number	Atomic Type	Coordinates (Angstroms)		
			X	Y	Z
1	53	0	3.594071	-0.065764	-0.199393
2	6	0	-2.815400	0.444486	0.004129
3	1	0	-3.102511	1.485131	0.058467
4	6	0	-3.758782	-0.523938	-0.020247
5	1	0	-3.433670	-1.551917	-0.075261
6	6	0	-1.372976	0.249931	-0.039099
7	6	0	-0.720142	-0.986525	-0.111284
8	6	0	0.664962	-1.070071	-0.151966
9	6	0	1.447760	0.074206	-0.122297
10	6	0	0.821790	1.309823	-0.049288
11	6	0	-0.560487	1.392912	-0.008333
12	9	0	-1.446254	-2.154545	-0.144753



13	9	0	1.251962	-2.303932	-0.223921
14	9	0	1.562802	2.458809	-0.018062
15	9	0	-1.162933	2.624592	0.063493
16	6	0	-5.202770	-0.320314	0.020241
17	6	0	-6.051792	-1.443821	-0.016162
18	1	0	-5.611845	-2.430919	-0.073456
19	6	0	-7.433887	-1.324542	0.019245
20	1	0	-8.034941	-2.219267	-0.010606
21	6	0	-8.053443	-0.053176	0.094116
22	6	0	-7.199638	1.080146	0.130371
23	1	0	-7.621747	2.070881	0.186843
24	6	0	-5.821090	0.944343	0.094390
25	1	0	-5.214024	1.838232	0.124517
26	7	0	-9.427339	0.079809	0.130609
27	6	0	-10.285126	-1.113994	0.087300
28	1	0	-10.131747	-1.687665	-0.832339
29	1	0	-11.326438	-0.800712	0.122893
30	1	0	-10.097961	-1.776759	0.938251
31	6	0	-10.041234	1.413822	0.211834
32	1	0	-9.731346	1.946560	1.116473
33	1	0	-11.123153	1.301595	0.238215
34	1	0	-9.782987	2.032073	-0.653959
35	6	0	8.426132	1.111776	-0.212974
36	6	0	6.881070	1.138421	-0.137096
37	7	0	6.273960	-0.223650	-0.337853
38	6	0	6.833682	-1.228779	0.631649
39	6	0	8.378402	-1.307150	0.572787
40	6	0	8.996112	0.095118	0.809524
41	1	0	6.561370	1.484496	0.847622
42	1	0	6.452952	1.808269	-0.882960
43	1	0	8.734455	0.826101	-1.223306
44	1	0	8.816993	2.113367	-0.017780
45	1	0	6.514806	-0.918029	1.628305
46	1	0	6.372892	-2.193040	0.416608
47	1	0	8.735186	-2.016224	1.323804
48	1	0	8.685474	-1.680902	-0.408796
49	1	0	8.751330	0.428970	1.822520
50	1	0	10.084121	0.047969	0.730962
51	1	0	6.441646	-0.536170	-1.290371

**Table 15.**

Optimized B3LYP/3-21G\*\* coordinates for dimer **1a-QUI**

Standard orientation:

Center Number	Atomic Number	Atomic Type	Coordinates (Angstroms)		
			X	Y	Z
1	53	0	-3.213329	0.058133	-0.014972
2	6	0	3.208707	0.467957	-0.013813
3	1	0	3.515291	1.504520	-0.011133
4	6	0	4.133803	-0.518346	-0.011342
5	1	0	3.789242	-1.541524	-0.014602
6	6	0	1.762033	0.298565	-0.018385
7	6	0	1.086766	-0.927838	-0.021192
8	6	0	-0.300275	-0.987941	-0.022599
9	6	0	-1.062738	0.170436	-0.021413
10	6	0	-0.414446	1.396628	-0.019849
11	6	0	0.970016	1.456346	-0.018363
12	9	0	1.791701	-2.109500	-0.021836
13	9	0	-0.909551	-2.213274	-0.024146
14	9	0	-1.134902	2.559205	-0.018594
15	9	0	1.595151	2.678995	-0.015891
16	6	0	5.581962	-0.341105	-0.003401
17	6	0	6.409111	-1.481517	-0.003744
18	1	0	5.949821	-2.461480	-0.010907
19	6	0	7.793723	-1.387895	0.004968
20	1	0	8.377514	-2.294567	0.004357
21	6	0	8.438224	-0.126731	0.014845
22	6	0	7.606489	1.023603	0.014971
23	1	0	8.047966	2.007521	0.022413
24	6	0	6.225116	0.913347	0.006094
25	1	0	5.635588	1.819467	0.007093
26	7	0	9.814861	-0.019120	0.024221
27	6	0	10.649364	-1.230231	0.023763
28	1	0	10.461504	-1.850029	0.906398
29	1	0	11.696817	-0.935954	0.031603

---

30	1	0	10.472417	-1.841654	-0.866911
31	6	0	10.455164	1.304896	0.035451
32	1	0	10.188657	1.890828	-0.850108
33	1	0	11.535180	1.172735	0.042381
34	1	0	10.176168	1.881727	0.923132
35	6	0	-8.483254	-0.245995	0.039176
36	6	0	-8.034007	1.047112	-0.690492
37	6	0	-6.463753	1.089314	-0.710758
38	7	0	-5.886245	-0.099284	0.009599
39	6	0	-6.371913	-0.108428	1.433822
40	6	0	-7.937339	-0.222100	1.490753
41	1	0	-6.075953	1.067196	-1.728616
42	1	0	-8.428024	1.052280	-1.708616
43	1	0	-8.433002	1.920795	-0.171477
44	1	0	-8.361819	0.625905	2.031780
45	1	0	-6.018952	0.811401	1.898949
46	1	0	-5.889470	-0.947411	1.934048
47	1	0	-8.234962	-1.134551	2.011227
48	1	0	-6.080321	1.983377	-0.220550
49	6	0	-6.324127	-1.363929	-0.678803
50	1	0	-5.910353	-1.343384	-1.686315
51	1	0	-5.869471	-2.195665	-0.141892
52	6	0	-7.891057	-1.473881	-0.701608
53	1	0	-8.256574	-1.494747	-1.730148
54	1	0	-8.215922	-2.393508	-0.211082
55	1	0	-9.572232	-0.307940	0.051443

---